Bacterial cellulose-collagen nanocomposite for bone tissue engineering

JOURNAL OF MATERIALS CHEMISTRY, CAMBRIDGE, v. 22, n. 41, supl. 1, Part 8, pp. 22102-22112, 39387, 2012

Journal of Materials Chemistry

Cite this: J. Mater. Chem., 2012, 22, 22102

www.rsc.org/materials

PAPER

Bacterial cellulose-collagen nanocomposite for bone tissue engineering

Sybele Saska,*[a] Lucas Novaes Teixeira,[b] Paulo Tambasco de Oliveira,[b] Ana Maria Minarelli Gaspar,[c] Sidney José Lima Ribeiro,[a] Younès Messaddeq[a] and Reinaldo Marchetto[a]

Received 12th June 2012, Accepted 3rd September 2012
DOI: 10.1039/c2jm33762b

A nanocomposite based on bacterial cellulose (BC) and type I collagen (COL) was evaluated for *in vitro* bone regeneration. BC membranes were modified by glycine esterification followed by cross-linking of type I collagen employing 1-ethyl-3-(3-dimethylaminopropyl)-carbodiimide. Collagen incorporation was studied by spectroscopy analysis. X-Ray diffraction showed changes in the BC crystallinity after collagen incorporation. The elastic modulus and tensile strength for BC-COL decreased, while the strain at failure showed a slight increase, even after sterilization, as compared to pristine BC. Swelling tests and contact angle measurements were also performed. Cell culture experiments performed with osteogenic cells were obtained by enzymatic digestion of newborn rat calvarium revealed similar features of cell morphology for cultures grown on both membranes. Cell viability/proliferation was not different between BC and BC-COL membranes at day 10 and 14. The high total protein content and ALP activity at day 17 in cells cultured on BC-COL indicate that this composite allowed the development of the osteoblastic phenotype *in vitro*. Thus, BC-COL should be considered as alternative biomaterial for bone tissue engineering.

1. Introduction

Cellulose obtained from plants has been widely used as biomaterial, such as hemostatic agents.[1] The production of pure cellulose involves elaborate and polluting processes of extraction and purification and therefore alternative methods of obtaining cellulose would be of great interest. Bacterial cellulose (BC) over the years has been an alternative for applications in the development of biomaterials. BC is obtained from cultures of the Gram-negative bacteria *Gluconacetobacter xylinus*, which produces highly hydrated membranes (up to 99% water), free of lignin and hemicelluloses as well as other biogenic products, and which present higher molecular weight and crystallinity than plant cellulose. BC membranes are characterized by a 3-D structure consisting of an ultrafine network of cellulose nanofibers ("nanocelluloses"). In addition, as compared to plant cellulose and other natural resorbable polymers such as collagen and chitosan, BC membranes have presented improved mechanical properties, which are essential for barrier membranes and scaffolds in tissue regeneration.[2–4]

Despite its excellent biological properties for tissue regeneration, mainly for the treatment of chronic wounds and burn wounds,[2,3,5] several studies have aimed to improve the biological properties of BC. In this way BC-collagen (BC-COL) composites have been developed for potential tissue engineering applications. Collagen not only plays the role of a physical material to support cell proliferation, but also enhances cell adhesion, proliferation and function.[4] BC-collagen composites are basically prepared by two processes. The first one includes the addition of type I collagen to the culture medium during cultivation of the bacterial strain, *Gluconacetobacter xylinus*.[5,6] The second process includes cyclic immersion of the wet BC pellicle in a collagen solution followed by a freeze-drying process.[4] In these two methodologies of collagen incorporation, the bonds between the collagen molecules and the cellulose are not covalent. In this first process, collagen was incorporated to BC during the process of the production of cellulose fibers by bacteria into the culture medium, which restricts the uniformity in terms of the amount of collagen incorporated into the cellulose fibers. Thus, the homogeneity of the composite is questionable due to the fact that the amount of collagen is determined by the metabolism of the bacteria, making it impossible to standardize these methodologies in terms of the collagen content in the composite. This standardization is crucial, since the ultimate goal of these products is applications *in vivo*.

Furthermore, the methods of purification of these BC-COL composites that have been used are also questionable.

[a]*Institute of Chemistry, Univ. Estadual Paulista – UNESP, Postal Code 355, Araraquara, São Paulo, Brazil. E-mail: sybele_saska@yahoo.com.br; sidney@iq.unesp.br; younes.messaddeq@copl.ulaval.ca; marcheto@iq.unesp.br; Fax: +55 16 3301-9636; Tel: +55 16 3301-9631*
[b]*Cell Culture Laboratory, Faculty of Dentistry of Ribeirão Preto, University of São Paulo – USP, Av. do Café s/n, CEP 14040-904, Ribeirão Preto, São Paulo, Brazil. E-mail: novaesrp@yahoo.com.br; tambasco@usp.br*
[c]*Dental School, Univ. Estadual Paulista – UNESP, Department of Morphology, Rua Humaitá, 1680, 14.801-903, Araraquara, São Paulo, Brazil. E-mail: anamaria@foar.unesp.br*

Purification techniques employing NaOH[6] or sterilization by autoclaving[5] denature collagen molecules in the composites due to the high pH and high temperature, respectively. In addition, sterilization by autoclaving cannot eliminate any residual bacteria present in the BC pellicle.

Therefore, in view of the importance of such composites in current medicine, and the disadvantages presented by known methods in the literature, searches for more effective and economically viable alternative composites is increasing. Our aim was to develop a composite based on BC and collagen for tissue engineering applications with collagen covalently and homogeneously incorporated into the BC; moreover, the amount of incorporated collagen can be controlled, and consequently, the incorporation of collagen into the composite is standardized.

2. Experimental

2.1 Synthesis of BC

Bacterial cellulose (BC) membranes were obtained from cultures of wild strains of *Gluconacetobacter xylinus*. *G. xylinus* was cultivated in 20 mL of medium in 100 mL flasks for 120 h at 28 °C in static culture. The nutrient medium contained 2 wt% glucose, 0.5 wt% peptone, 0.5 wt% yeast extract, 0.27 wt% disodium hydrogen phosphate, and 0.115 wt% citric acid. Bacterial cellulose pellicles that formed during that time at the air/liquid interface were harvested, and purified by immersion in a 2 wt% NaOH solution at 80 °C for 1 h; subsequently the pellicles were immersed in a 1 wt% NaClO solution for 30 min. These pellicles were then washed with deionized water and sterilized (120 °C for 15 min). Highly hydrated BC membranes were cut to a standard size, 25 mm in diameter and 5 mm thickness.

Dried BC membranes were obtained by drying at 50 °C and sterilized by gamma radiation (20 kGy). These membranes were used as a control.

2.2 Preparation of BC-COL nanocomposites

The preparations of the BC-COL composites was performed following the methodology proposed before.[7] The incorporation of collagen (COL) (type I collagen from rat tail tendon – Sigma®, Saint Louis/EUA) into the BC hydrogel was initiated by the exchange of water in the highly hydrated BC by dimethylformamide (DMF) (Synth®) by vacuum filtration. The BC surface was then modified by Fmoc-glycine (Fmoc-Gly) esterification to the free hydroxyl groups of BC, through a solid-phase synthesis strategy employing Fmoc-based chemistry (9-fluorenylmethyloxycarbonyl – Fmoc). For this reaction, a solution was prepared containing 238 mg Fmoc-Gly, 162 mg 1,1′-cabonyldiimidazole (CDI) (Sigma®), 127 μL *N*-methylimidazole (NMI) (Fluka®) and 8 mL DMF for each sample. The esterification reaction was carried out under shaking at room temperature (RT) for 2 h. After the esterification reaction, the samples were washed twice with DMF by vacuum filtration and were then soaked in DMF for 24 h for the removal of excess reagents.

Quantitative analysis by ultraviolet-visible spectroscopy (UV/VIS, SHIMADZU UV-1601PC; detection at 290 nm) was used to determine the incorporation degree (IG) of Fmoc-Gly to the OH groups of BC. The measurements were performed using very small samples of BC-Fmoc-Gly (~30 mg), thus the samples were weighed after being soaked in piperidine in DMF (20%) into a quartz cuvette (10 × 10 mm) for 10 min. Next, the solutions were mixed and the absorbance was measured. The incorporation degree (IG) of amino acids was calculated using the equation as follows:

$$\mathrm{IG\ (mmol/g)} = \frac{(\text{sample Absorbance}) - (\text{reference Absorbance})}{1.65 \times \text{weight of sample (mg)}}$$

Deprotection of BC-Gly-Fmoc was carried out using piperidine in DMF (20%) at RT for 2 h, followed by successive washes with DMF under vacuum to remove the excess piperidine solution. Next, the exchange of DMF for deionized water in the BC-Gly samples was carried out by vacuum filtration in a porous plate filter until excess DMF was removed.

Then, each BC-Gly sample in water was soaked in 10 mL of aqueous collagen solution at 4 °C for 24 h (pH 6). This solution contained 600 μL type I collagen (4 mg mL^{-1}) and 5 mmol L^{-1} 1-ethyl-3-(3-dimethylaminopropyl) carbodiimide (EDC) (Novabiochem®), used for cross-linking, improving the biostability of the membrane. The samples were washed with deionized water under vacuum to remove excess reagents. BC-COL samples were dried into moulds at 37 °C and sterilized by gamma radiation (20 kGy).

2.3 Characterization of BC-COL nanocomposites

Scanning electron microscopy (SEM) images were obtained with a Philips XL 30 scanning electron microscope. The samples were sputter coated with a 1 nm thick gold layer for 60 s (3 kV and 9.5 μA). The morphology was observed at an accelerating voltage of 10 kV. X-Ray diffraction (XRD) patterns of BC and BC-COL were performed on a Kristalloflex Simens Diffractometer with a Ni filter and Cu Kα radiation from 4° to 70°. Fourier transform infrared (FT-IR) spectra were obtained with dried powdered samples on a Perkin Elmer Spectrum 2000 Fourier transform infrared spectrophotometer. Pellets were prepared from mixtures of the samples and KBr (1 : 100 in weight). Thirty-two scans were accumulated at a resolution of 4 cm^{-1}. The Raman spectra of BC and BC-COL membranes were acquired using a Lab RAM HR 800 spectrometer (Horiba Jobin Yvon) coupled to a CCD camera (Horiba Jobin Yvon) as detector. A He–Ne laser operating with an excitation line of 632.81 cm^{-1} and maximum power of 15 mW was applied as the light source for the excitation of Raman scattering. The spectra were recorded over the range of 4000–100 cm^{-1} using an operating spectral resolution of 4 cm^{-1}. The spectra were averaged over five scans with an acquisition time of 200 s per scan. The thermogravimetric (TG) curves of the dried samples were recorded using a TA SDT 2960 from TA Instruments Co. The samples were heated in open α-alumina pans from 25 to 600 °C under a nitrogen atmosphere (flow rate: 70 mL min^{-1}) at a heating rate of 10 °C min^{-1}.

2.4 Swelling tests

BC and BC-COL membranes, sterilized by gamma radiation or not, were separately immersed in distilled water at RT for 4 h. The samples were removed at certain times, initially at 1 and

5 min, followed by measurements every 5 min until 30 min, and then measured every 15 min until a total of 4 h. After removal from the distilled water, they were laid on a filter paper for removal of excess superficial water and then were weighed. The content of the distilled water in the swollen membranes was calculated by the following equation: water uptake (%) = $[(W_s - W_d)/W_s] \times 100$, where W_d is the weight of the dry membrane and W_s is the weight of the swollen membrane, respectively. All experiments were performed three times per sample. Data were expressed as mean ± SE. The Kruskal–Wallis test was applied. BioEstat statistical package v.5 was used (UFPA, Belém, Brazil) to perform the tests (p-value $p < 0.05$ was defined as a significant difference).

2.5 Contact angle measurements

Measurements were performed using the sessile drop method on a Dataphysics Contact Angle System (KSV Instruments LTD, Finland), equipped with a CCD camera. The sessile drop was dispensed by a syringe pump through a flat tip needle 0.5 mm in diameter. Deionized water (10 μL) was gently dropped on each piece of membrane. Static contact angles were measured 10 s after placing the drop of deionized water onto the sample surface at room temperature. The captured images of sessile drops were analyzed using drop-shape analysis SCA20 software. All experiments were conducted under ambient conditions and were performed three times per sample.

2.6 Mechanical testing

Mechanical properties, including tensile strength, elastic modulus and strain at failure were carried out on a MTS-810 testing machine (Material Test System-MTS 810; MTS System Corporation) equipped with Test Satr II software, with a 10 kN load cell and a tensile force applied at an extension rate of 0.5 mm min^{-1}. The membranes with thickness in the range of 20 μm for BC and 70 μm for BC-COL were cut into regular rectangular shapes with an inner width of ~6.50–7.50 mm. At least five specimens were tested for each condition. Before measurements, the samples were soaked in simulated body fluid (SBF)[8] for 10 min at RT and then laid on filter paper for removal of excess superficial water before carrying out the mechanical tests. The tensile strength was determined as the maximum point of the force–strain curve.

2.7 Cell culture experiments

2.7.1 Cell isolation and primary osteogenic cell cultures. Osteogenic cells were isolated by sequential trypsin/collagenase digestion of calvarial bone from newborn (2–4 days) *Wistar* rats, as previously described.[9–12] All animal procedures were in accordance with the guidelines of the Animal Research Ethics Committee of the University of São Paulo. Cells were seeded on BCγ and BC-COLγ membranes at a cell density of 2×10^4 cells per well and cultured for periods of up 21 days using Gibco α-Minimum Essential Medium with L-glutamine (Invitrogen®, Carlsbad, CA) supplemented with 10% fetal bovine serum (Invitrogen®), 7 mmol L^{-1} β-glycerophosphate (Sigma®, St Louis, MO), 5 μg mL^{-1} ascorbic acid (Sigma®), and 50 μg mL^{-1} gentamicin (Invitrogen®), at 37 °C in a humidified atmosphere with 5% CO_2. The culture medium was changed every three days. The progression of cultures was examined by phase contrast microscopy of cells grown on polystyrene.

2.7.2 Cell morphology. At days 1, 3, and 7, cell cultures were fixed for 10 min at RT using 4% paraformaldehyde in 0.1 mol L^{-1} sodium phosphate buffer (PB), pH 7.2. After being washed in PB, cells were processed for fluorescence labeling for the detection of actin cytoskeleton and cell nuclei. Briefly, they were permeabilized with 0.5% Triton X-100 in PB for 10 min, followed by blocking with 5% skimmed milk in PB for 30 min. Alexa Fluor 488 (green fluorescence)-conjugated phalloidin (1 : 200, Molecular Probes, Eugene, OR) was used to label the actin cytoskeleton. Before microscope observation, the samples were briefly washed with deionized water (dH_2O), and the cell nuclei were stained with 300 nmol L^{-1} 4′,6-diamidino-2-phenylindole, dihydrochloride (DAPI, Molecular Probes) for 5 min. The membranes were placed face up on glass slides, covered with 12 mm round glass coverslips (Fisher Scientific) and mounted with an antifade kit (Vectashield, Vector Laboratories, CA). The samples were then examined under epifluorescence, using a Leica DMLB light microscope (Leica, Germany), with N Plan (X10/0.25, X20/0.40) and HCX PL Fluotar (X40/0.75, X100/1.3) objectives, outfitted with a Leica DC 300F digital camera. Acquired digital images were processed with Adobe Photoshop software (Adobe Systems).

2.7.3 Cell viability/proliferation. Cell viability/proliferation was evaluated by the 3-[4,5-dimethylthiazol-2-yl]-2,5-diphenyl tetrazolium bromide (MTT, Sigma®) assay.[13] At day 10 and 14, cells were incubated with 10% MTT (5 mg mL^{-1}) in culture medium at 37 °C for 4 h. The medium was then aspirated from the well, and 1 mL of acid isopropanol (0.04 mol L^{-1} HCl in isopropanol) was added to each well. The plates were then stirred on a plate shaker for 5 min, and 150 μL of this solution was transferred to a 96-well format using opaque-walled transparent-bottomed plates (Fisher Scientific). The optical density was read at 570–650 nm on a plate reader (μQuant, Biotek, Winooski, VT), and data were expressed as absorbance.

2.7.4 Total protein content. The total protein content is a general indicator of the interfacial tissue formation on the biomaterial surface, and reflects cell proliferation activity and extracellular matrix production.[14,15] In addition, in the present study total protein values were also used to normalize ALP activity.[16]

Total protein content was determined at days 14 and 17 using a modification of the Lowry method.[14] The wells were filled with 2 mL 0.1% sodium lauryl sulphate (Sigma®). After 30 min, 1 mL of the sample from each well was mixed with 1 mL of Lowry solution (Sigma®) and left for 20 min at RT. Subsequently, 0.5 mL of the phenol reagent of Folin and Ciocalteau (Sigma®) was added and the resulting solution left for 30 min at RT, after which the absorbance was measured using a spectrophotometer (CE3021-Cecil, UK) at 680 nm. Total protein content was calculated from a standard curve using bovine serum albumin (Sigma®), giving a range of 25 to 400 μg protein mL^{-1} and data were expressed as μg protein mL^{-1}.

2.7.5 Alkaline phosphatase activity. Alkaline phosphatase (ALP) activity was assayed in the same lysates used for determining total protein content as the release of thymolphthalein from thymolphthalein monophosphate using a commercial kit (Labtest Diagnostica, Brazil). Briefly, 50 mL of thymolphthalein monophosphate was mixed with 0.5 mL of diethanolamine buffer (0.3 mmol mL^{-1}, pH 10.1) and left for 2 min at 37 °C. The solution was added to 50 mL of the lysates obtained from each well for 10 min at 37 °C. For color development, 2 mL of 0.09 mol L^{-1} Na_2CO_3 and 0.25 mol L^{-1} NaOH were added. After 30 min, absorbance was measured at 590 nm, and ALP activity was calculated from a standard curve using thymolphthalein to give a range of 0.012–0.4 μmol thymolphthalein h^{-1} mL^{-1}. Data were expressed as ALP activity normalized by the total protein content.

2.7.6 Mineralized matrix formation. Mineralized matrix formation was detected at day 21 by Alizarin Red S (Sigma®), which stains areas rich in calcium. Cultures were fixed in 10% formalin for 2 h at RT. After fixation, the specimens were dehydrated through a graded series of alcohols and stained with 2% Alizarin Red S (Sigma®), pH 4.2, for 10 min. The calcium content was evaluated using a colorimetric method.[17] Briefly, 280 μL of 10% acetic acid was added to each well containing the membranes stained with Alizarin Red S, and the plate was incubated at RT for 30 min under shaking. This solution was transferred to a microcentrifuge tube and after vortexing for 1 min, the slurry was overlaid with 100 μL of mineral oil (Sigma®), heated to 85 °C for 10 min, and transferred to ice for 5 min. The slurry was then centrifuged at 20 000× *g* for 15 min and 100 μL of supernatant was transferred to a new microcentrifuge tube. Then, 40 μL of 10% ammonium hydroxide was added to neutralize the acid and this solution containing 140 μL was read at 405 nm in 96-well format using opaque-walled transparent-bottomed plates (Fisher Scientific) on a μQuant (Biotek) plate reader. Data were expressed as absorbance.

3. Results and discussion

3.1 Characterization

The standardization in the processes of purification and sterilization of the bacterial cellulose membranes is no doubt, important. Moreover the standardization in the determination of the amount of incorporated collagen for the development of medical devices must be taken into account. In this study a methodology was developed to optimize the process of standardization of the amount of incorporated collagen. Thus, the homogeneity of the composite was observed by the SEM images and the amount of collagen was determined by thermogravimetric analysis (TGA), other characterization techniques contributed to understanding the formation of the composite.

Fig. 1 shows typical SEM images of dried BC and BC-COL membranes. Fig. 1A shows a well-organized three-dimensional (3D) structure for dried BC; moreover, the BC film presents irregular interconnected pores. Fibers are about 11 to 56 nm in size (average 27 nm). The SEM image of the surface morphology of BC-COL composite (Fig. 1B) shows that collagen filled and homogeneously covered the BC membrane structure. The

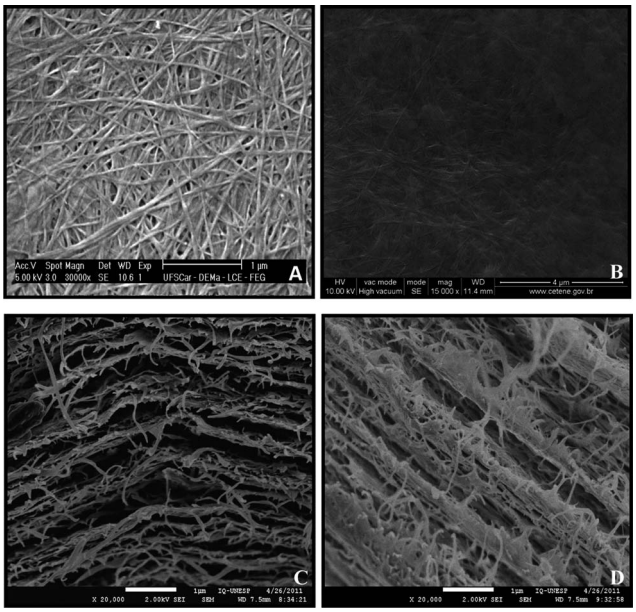

Fig. 1 SEM surface images of the BC membrane and BC-COL composite (A and B) at 30 000× and 15 000×, respectively; SEM cross-section images of the BC membrane (C) and BC-COL composite (D) at 20 000×.

methodology employed for obtaining BC-COL composite promoted a compact surface with the filling of surface pores. This is an important feature for a membrane for tissue regeneration, especially when the membrane is used for guided bone regeneration since the membrane can be used as a physical barrier. Thus, the BC-COL membrane could favor the function of cell occlusion excluding the surrounding soft tissues and also protect the blood clot in the bone defect better than BC membrane. In the SEM cross-section image (Fig. 1C), BC fibers oriented in layers may be observed. In Fig. 1D, SEM image BC fibers covered with collagen and also oriented in layers are observed. It is to be noted that the BC-COL composite presents a well-interconnected layer structure and a large surface area necessary for cellular attachment, and vascularization as BC; however BC and BC-COL can have potential to be employed in preparing the scaffolds. In other words, these materials, when used as a tissue regeneration scaffold can potentially promote cellular ingrowth, and when used as a membrane could be excellent material for guided bone regeneration, mainly the BC-COL composite.

The XRD patterns obtained for BC, BC-COL composite and pure collagen are shown in Fig. 2. The peaks for BC [Fig. 2(a)] were identified as native cellulose (PDF#50-2241 ICDD, PDF-2, International Centre for Diffraction Data, Power Diffraction File-2) and the characteristic peaks observed at $2\theta = 15°$ and 22.5° were attributed to the cellulose 1α and 1β phases, respectively.[18] The sharp peaks indicated that the bacterial cellulose was semi-crystalline, which had previously been reported.[2] Fig. 2(b) shows a broad peak in the 2θ range of 15–35° which is typical for pure collagen.[6,19] The diffraction pattern presented in Fig. 2(c) shows a peak at $2\theta = 16.8°$. Moreover, a decrease in the intensity of the BC is observed that must be related to the presence of collagen added to the BC structure.

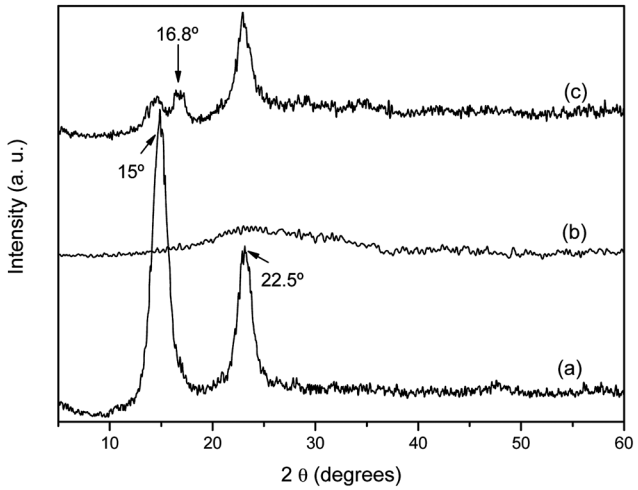

Fig. 2 X-Ray diffraction patterns of the BC (a), freeze-dried pure collagen (b) and BC-COL composite (c). The characteristic peaks are indexed at the top for BC and BC-COL samples.

Fig. 3 shows the FT-IR spectra of the BC, BC-Gly, BC-COL samples and freeze-dried pure collagen. Typical IR bands for cellulose were observed in Fig. 3A(a): OH stretching at 3450 cm^{-1}, CH stretching for the alkanes and CH_2 asymmetric stretching at ~2900 cm^{-1}, CH_2 symmetric stretching at 2700 cm^{-1}, H–O–H bending of adsorbed water at 1645 cm^{-1}, CH_2 deformation at 1432 cm^{-1}, CH_3 deformation at ~1370 cm^{-1}, OH deformation at ~1332 cm^{-1} and in the region 1320–1030 cm^{-1} characteristic C–O deformation.[18] Fig. 3A(b) shows typical IR bands for pure collagen: OH stretching at 3430 cm^{-1}, N–H stretching at ~3060 cm^{-1} for the amide A, CH_2 asymmetric stretching at ~2900 cm^{-1}, C=O stretching at 1660 cm^{-1} for the amide I, N–H deformation at 1545 cm^{-1} for the amide II, N–H deformation at 1240 cm^{-1} for the amide III bands.[20]

A band in the region of around 3500 cm^{-1} was observed in all IR spectra, but with decreasing intensity for the BC-Gly and BC-COL samples. Hydrogen bonding between amino acids (glycine) and OH groups of BC would in fact lead to a decrease of the 3500 cm^{-1} band. Moreover, comparing just BC-Gly and BC-COL, smaller intensity for that band is observed for the BC-Gly sample, suggesting that the collagen was bonded to the OH groups of the BC-Gly that were still free through the effects of EDC cross-linking. A band at ~2900 cm^{-1} also was observed in all IR spectra, but was more intense in the BC spectrum, suggesting that both glycine and collagen were bonded to the CH groups by hydrogen bonding, whereas in the BC-COL spectrum we observed a more intense decrease of this band in relation to the same band of the BC-Gly spectrum. The interaction between BC and collagen was confirmed by the fact that the band at 1645 cm^{-1} in the spectrum of BC shifted to 1656 cm^{-1} in the spectrum of the BC-COL composite (Fig. 3B). Furthermore, the bands at around 1420 and 1320–1210 cm^{-1}, which are attributed to C–O deformation of carboxylic acids or COO– symmetric stretching of free amino acids, were observed in the three samples containing BC. Note that the intensity of these bands decreased with the presence of glycine and collagen, suggesting formation of the BC-Gly sample and the BC-COL composite.

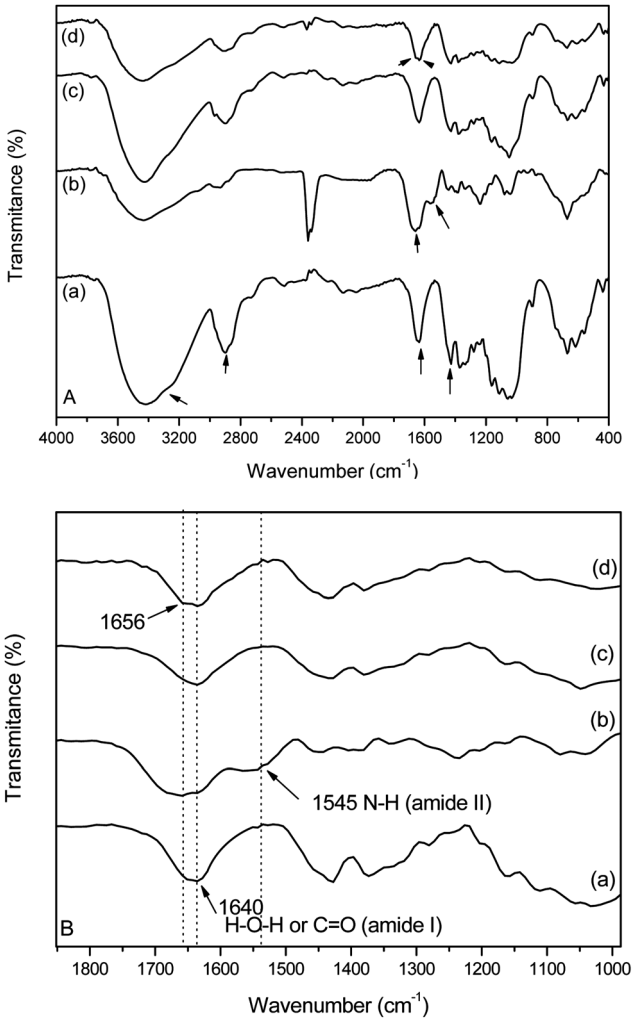

Fig. 3 FTIR spectra: (A) BC (a), freeze-dried pure collagen (b), BC modified with amino acid (c) and BC-COL composite (d); (B) FTIR spectra around 1800–1000 cm^{-1}, amide II and III bands (arrow indicated); the spectrum of BC-COL membrane shows red shift at 1656 cm^{-1} (d) compared to the band at 1640 cm^{-1} of the spectrum BC (a).

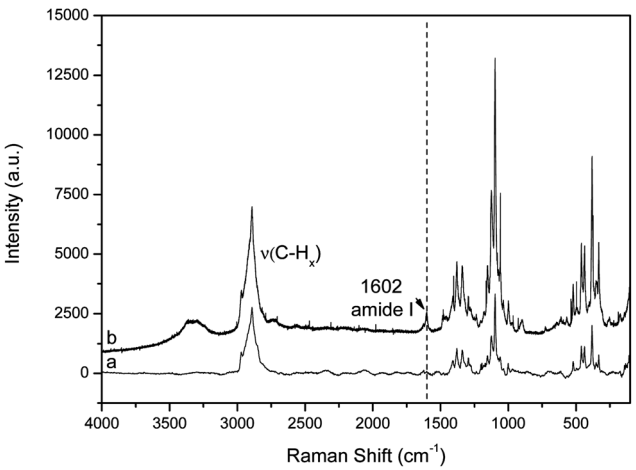

Fig. 4 Raman spectra of samples: BC (a), BC-COL composite (b).

Fig. 4 represents two spectral regions of the Raman spectra of the BC and BC-COL showing scattering behavior. Typical spectral peaks attributed to cellulose were observed at about 380, 437, 461, 521 cm^{-1} for heavy atom stretching, at 1096 and 1125 cm^{-1} for atoms stretching and at 1380 cm^{-1} for HCC, HCO and HOC bending[21] which were observed in the spectrum of the BC membrane. In addition, this Raman spectrum was characteristic of the vibrational behaviour of crystalline cellulose I related to bacterial cellulose.[22] Spectrum (b), Fig. 4, showed the presence of a characteristic band of C=O stretching at about 1600–1620 cm^{-1} for amide I,[23] confirming the presence of collagen incorporated onto BC fibers. The band at the region from 3400–3200 cm^{-1} could be assigned to cellulose hydroxyl groups and N–H stretching for the amide, which was observed to increase in relative intensity for the BC-COL membrane in comparison with pure BC membrane. This increase in intensity is suggested by incorporation of collagen into the BC network due to the presence of N–H groups. Furthermore, it was observed that the peak ~2890 cm^{-1} (CH stretching of CH_2) also showed an increase with the incorporation of collagen, suggesting that the presence of collagen molecules promotes CH_2 interaction.

The TG curves for BC, BCγ, BC-COL, and BC-COLγ membranes are shown in Fig. 5. Thermogravimetric analysis was carried out to estimate the thermal stability and degradation profiles of the BC, BCγ, BC-COL, and BC-COLγ membranes, as well as to measure the amount of collagen content. The BC and BCγ samples showed initial smooth weight loss from ambient temperature up to 250 °C (8%) due to water and solvent loss.[18,24] The BC-COL and BC-COLγ samples showed initial smooth weight loss from ambient temperature up to 250 °C (15%) due to water and solvent loss, in addition to collagen incorporated into BC. Important weight loss was observed at around 300 °C, which referred to decomposition of the cellulose of the samples BC (T_{onset} 289 °C) and BCγ (T_{onset} 308 °C); however, this important weight loss was observed at around 268 °C for the BC-COL (T_{onset} 267 °C) and BC-COLγ (T_{onset} 268 °C) samples.[25] These events could be associated with a cellulose degradation process including depolymerization, dehydration and decomposition of glucosyl units followed by formation of a charred residue.[18,25,26] Moreover, the onset temperature (T_{onset}) observed in the TG curves revealed that the thermal stability of BC decreased with the presence of collagen; the T_{onset} values observed for the BC-COL and BC-COLγ decreased by 22 and 40 °C, respectively, when these values were compared to the BC and BCγ samples, respectively. Therefore, sterilization slightly increased the thermal stability of BC membrane, but gamma radiation did not promote changes to the characteristic temperatures for the BC-COL composite. This behavior may be associated with the broken hydrogen bonds and reduced crystallinity of BC by the incorporation of collagen. Thus, lower crystallinity leads to decreased T_{onset} values,[27] corroborating the XRD data. These results permitted us to conclude that gamma radiation is an adequate treatment for sterilization, since it did not change of the thermal stability of the composite.

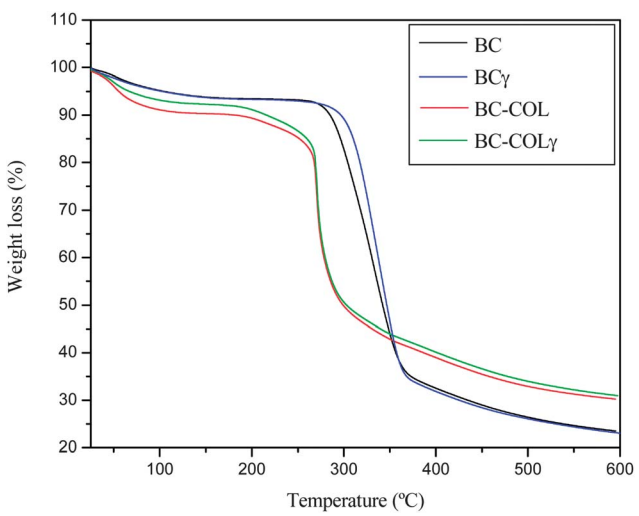

Fig. 5 Typical TG curves for the BC and BC-COL membranes before and after sterilization by 20 kGy gamma radiation (γ).

A carbonaceous residue was observed for the pure BC and BCγ membranes around 23.5% at 600 °C. Therefore, BC-COL and BC-COLγ composites presented a residue of around 31% at 600 °C confirming the incorporation of collagen into BC membrane, which means that the collagen content was around 6.5%. Compared to the literature, Wiegand *et al.*,[5] developed BC-collagen composite, but the collagen was bound to the lower side of the bacterial cellulose pellicle during the formation process and the authors affirmed that collagen was not evenly distributed. However, CHN analysis showed high nitrogen content in the BC-collagen composite (6%), which rate is similar to our BC-COL composite developed. Other studies did not measure the collagen content.[4,6] Furthermore, the methods of purification of these composites based on BC and collagen that have been used are also questionable. Purification techniques employing NaOH[6] or sterilization by autoclaving[5] denature collagen molecules in the composites due to the high pH and high temperature, respectively. In addition, only sterilization by autoclaving cannot eliminate any residual bacteria present in the BC pellicle. Thus, incorporation of collagen after purification of the BC membranes with NaOH solution is the most appropriate methodology to ensure the structure integrity of the collagen molecules. Therefore, the BC-COL composites only were sterilized by gamma radiation after the end of the materials' development. TGA showed that gamma radiation is an adequate treatment for sterilization.

3.2 Degree of swelling and contact angle measurements

The results for the degree of swelling for BC and BC-COL membranes with and without sterilization by gamma radiation (γ) are shown in Fig. 6. After 4 h, the water uptake ability of the BC and BC-COL membranes was 160 and 206%, respectively. All membranes absorbed water within 1 min and the BC and BCγ membranes were saturated within 1 h; the BC-COL and BC-COLγ membranes were saturated within 3 h. The water uptake of membranes slightly decreased with sterilization by gamma radiation, but the difference was not statistically significant ($P = 0.082$). The swelling or hydrophilic property of membranes showed a slight increase with the incorporation of collagen, but again the difference was not statistically significant. Thus, the swelling behavior of the BC-COLγ membrane suggested that a decrease in water uptake may be related to

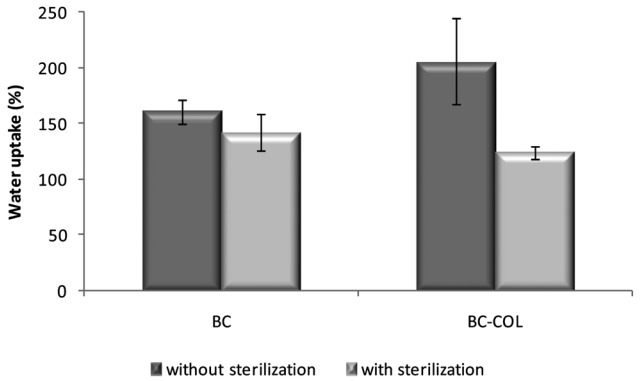

Fig. 6 Water uptake of BC and BC-COL membranes without and with sterilization by gamma radiation ($t = 4$ h). Data are reported as mean ± SE; $p > 0.05$.

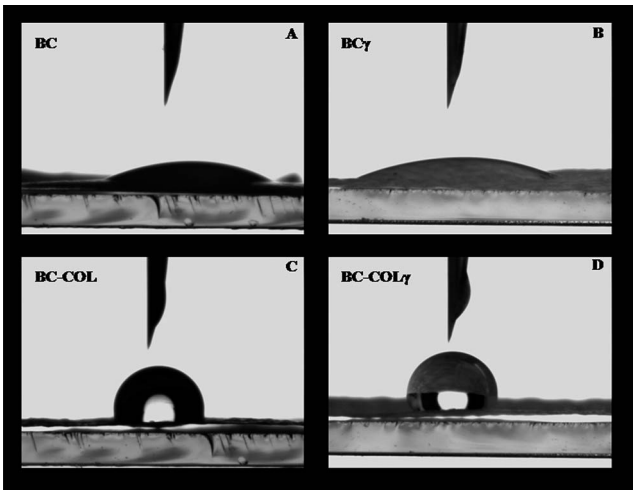

Fig. 7 Changes in surface wettability after collagen incorporation and sterilization. (A) BC membrane ($t = 10$ s); (B) the slightly increased hydrophobicity for BCγ membrane compared to BC ($t = 10$ s); (C) BC-COL membrane ($t = 10$ s); (D) the measured contact angle for BC-COLγ membrane did not change for this membrane when compared to BC-COL membrane ($t = 10$ s).

cross-linking promoted by the chemical agent (EDC), and mainly by the physical agent (gamma radiation). Moreover, the gamma radiation promoted a decrease in the water percentage of the composites as observed in Fig. 5, in addition to decreasing the free groups such as hydroxyl and carboxylic groups in the sample.

The contact angle measurements for BC and BCγ membranes showed that these membranes were hydrophilic (Table 1); however, when collagen was incorporated into the BC network, its surface hydrophobicity increased significantly (Fig. 7); gamma radiation did not significantly change the surface hydrophobicity of the BC-COL membrane at 10 s.

The decrease in surface hydrophilicity of the samples after sterilization may have been due to the decrease of the free surface hydroxyl and carboxylic groups, suggesting that the cross-linking of collagen fibrils also was promoted by the action of gamma radiation. According to the literature, more effective cross-linking of collagen fibrils lowers the swelling ratio of the material.[28,29] Thus, there is a change in the distribution of charge in the collagen molecule, influencing the hydrophilic properties of the material. These data corroborate those observed with the water uptake ratio shown in Fig. 6. In addition, these data revealed that the decrease in hydroxyl and carboxylic groups was uniform, since the cross-linking reaction occurred on the surface as well as inside BC-COL composite, suggesting that cross-linking of collagen was efficient employing EDC and gamma radiation.

3.3 Mechanical testing

Fig. 8 shows the typical stress–strain curves for each type of membrane. All of the membranes exhibited a similar stress–strain pattern, that is, the stress increased linearly (elastically) with respect to the strain. The results revealed that incorporation of collagen into the BC network decreased the tensile strength and elastic modulus, but increased the strain at failure.

Table 1 Contact angle measured of the BC and BC-COL membranes with and without sterilization by gamma radiation (20 kGy). The values indicated represent mean ± error standard, where $n = 3$

Membranes	$T = 0$ s	$T = 10$ s
BC	22 ± 3.2	15.7 ± 0.8
BCγ	31.1 ± 0.8	25.8 ± 4.4
BC-COL	105.7 ± 4.3	101 ± 2.5
BC-COLγ	114.3 ± 2.0	103.3 ± 3.8

The mechanical properties of the membranes, such as their tensile strength, elastic modulus, and strain at failure, are summarized in Table 2.

According to the results, we observed lower elastic modulus and higher strain at failure of the membranes (Fig. 8). Furthermore, the stress–strain curves for BC-COL and BC-COLγ showed an increase in the strain at failure, in spite of the decrease in their tensile strength and elastic modulus as compared BC and BCγ, respectively. This suggests that the presence of collagen in the BC network promoted better flexibility than in BC membranes even after sterilization, thus facilitating their manipulation in surgical applications.

Studies have shown that the tensile strength of collagen increases as cross-linking increases;[29,30] as a result, the percent elongation is decreased. However, the decrease in the percent elongation observed for the BC-COLγ membrane was related to the BC network and not to the collagen molecule, because the BC membrane showed a decrease of 4% compared to BCγ, and this pattern was also maintained for the BC-COLγ membrane (Table 2).

In addition, the BC-COLγ membrane showed extremely high values for tensile strength, elastic modulus and strain at failure as compared with data in the literature, on average eight times higher for tensile strength.[29,30] Zhijiang and Guang[4] developed a BC-collagen composite which presented higher values for tensile strength and elastic modulus as compared with BC-COLγ membrane with these values were related to BC network (200 MPa, tensile strength). In this study, after sterizalition BC network showed 83 MPa tensile strength, see Table 2; in addition, the composites of these authors showed a lower strain at failure than the BC-COLγ membrane. Thus, lower values for

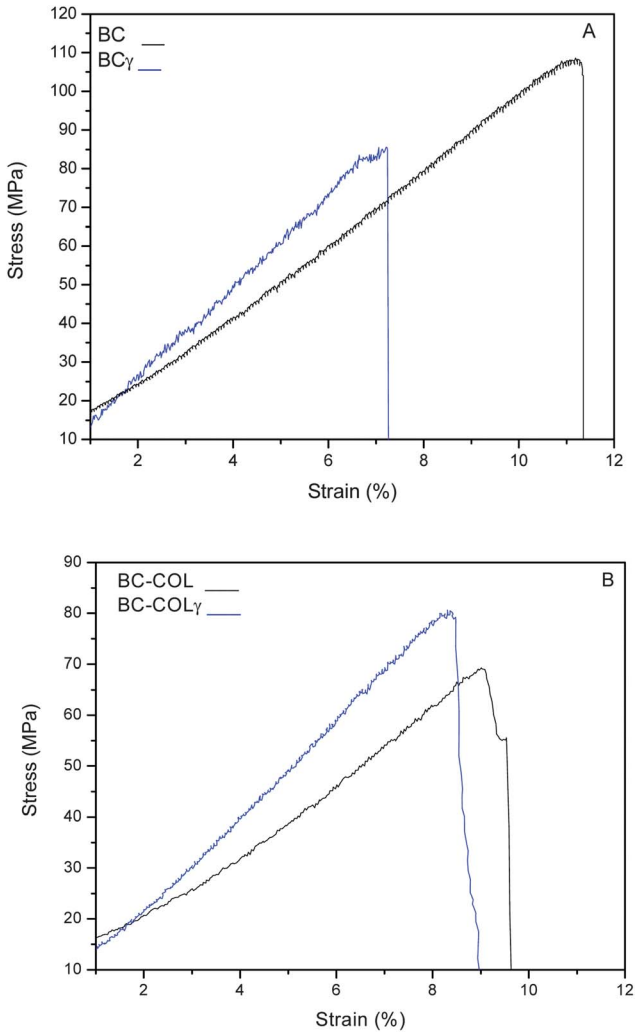

Fig. 8 Typical stress–strain curves for the BC and BCγ (A) membranes, and for the BC-COL and BC-COLγ composites (B).

Table 2 Mechanical properties of the BC and BC-COL membranes, with and without sterilization by gamma radiation (20 kGy). The values indicated represent mean ± error standard, where $n = 5$

Membranes	Tensile strength (MPa)	Elastic modulus (GPa)	Strain (%)
BC	95.1 ± 4.6	0.9 ± 0.03	11.8 ± 0.5
BCγ	83.5 ± 6.0	1.13 ± 0.1	7.8 ± 0.8
BC-COL	76.7 ± 4.9	0.63 ± 0.11	14.5 ± 2.8
BC-COLγ	84.6 ± 4.8	0.88 ± 0.08	10.1 ± 1.1

tensile strength and elastic modulus found to BC-COLγ membrane are related to the type of BC membrane and not the composite.

Coïc *et al.*,[31] studied the mechanical properties of three commercial membranes for guided bone regeneration, and observed that the measurements for tensile strength, elastic modulus and strain at failure decreased when these membranes were moistened. The membranes studied were: (1) Biomend Extend®, whose values obtained for tensile strength, elastic modulus and strain at failure were 4 MPa, 20 MPa and 25%, respectively; (2) TBR®: whose values obtained for tensile strength, elastic modulus and strain at failure were 1.6 MPa, 10 MPa and 26%, respectively. Mechanical testing for Bio-Gide® membrane was carried out only on the dry membrane, and the results obtained for tensile strength, elastic modulus and strain at failure were 15 MPa, 105 MPa and 31.5%, respectively.[31] Based on these literature data, we conclude that BC served as an excellent template for the incorporation of collagen, and although a lower amount of collagen was used in the BC-COL composite as compared with the other studies, the BC-COL composite exhibited higher values in terms of its mechanical properties, mainly elastic modulus. In addition, these results revealed that the novel BC-COL composite developed in this study represented a great advance in relation to mechanical properties when collagen is used in the preparation of membranes for tissue regeneration.

3.4 Cell culture experiments

One current goal of tissue engineering is the development of polymer composites, metal-free, with mechanical properties comparable to hard or soft tissues for partial or total replacement/reconstruction of the organ or tissue to be repaired.

Composites from a combination of natural polymers (collagen, cellulose, polyhydroxybutyrate) or synthetic polymers [poly(lactic-*co*-glycolic acid), poly(lactic acid), poly(ε-caprolactone)] associated with bioceramics have been highlighted in tissue engineering[5,19,20,32–36] as being biocompatible, osteoconductive, bioactive and with satisfactory mechanical properties, in addition to being resorbable, therefore potential material for application in regenerative medicine therapies.

Collagen membranes developed in recent years have presented ideal physicochemical characteristics for clinical application.[29,37–40] According to literature sources, the determination of the density of cross-linking reaction directly influences physical properties of the collagen matrices, in other words, increasing cross-linking of collagen fibrils provides an increased tensile strength and enzymatic degradation, and higher thermal stability.[28,29,38,40]

A cross-linking agent has shown excellent results for cross-link of collagen fibrils is 1-ethyl-3-(3-dimethylaminopropryl) carbodiimide (EDC). EDC has been used to modify side-groups on proteins to make them reactive with other side-groups and to mediate the ester bond formation between the hydroxyl and carboxyl groups.[28] In contrast to conventional chemical agents such as glutaraldehyde or polyepoxides, carbodiimides do not remain as a part of linkage but simply change to water-soluble urea derivatives that have very low cytotoxicity.[41] If stable covalent linkages are produced, this method can preclude depolymerization and release of residual toxic reagent.[28,41]

Biomaterials developed for tissue engineering and/or tissue regeneration purposes should be non-hazardous, non-immunogenic and biologically capable of supporting cell attachment, spreading, proliferation, and differentiation.[42,43] Collagen or collagen-based materials have been extensively used in bone tissue engineering/regeneration, at least in part because collagen represents 90% of the bone organic matrix. Moreover, collagen incorporation into different substrates can create materials able to produce better tissue and cell responses, such as cell adhesion and

growth, and up-regulation of bone-associated genes, including type I collagen, osteopontin, and alkaline phosphatase.[44]

Studies concerning collagen membrane on guided bone regeneration (GBR) have reported satisfactory results *in vivo*. For example, the rate of bone regeneration has effectiveness similar to e-PTFE membrane, due to the advent of collagen membranes with good mechanical strength. In the past, it was hard to get results as satisfactory and predictable due to the difficulty of producing collagen membranes with these characteristics.[45,46]

BC membrane has several features that make it a suitable alternative to guided bone regeneration procedures.[3,4] Nevertheless, its association with other materials may provide improvement in its mechanical and biological properties.[47,48] As can be seen, a lower amount of collagen incorporated into BC membrane, mainly improved the strain at failure of the composite. According to literature, the composite based on CB-collagen[4–6] has some disadvantages in relation to the methodology of incorporation and uniformity of collagen, moreover inherent problems in the purification of BC membranes and sterilization of composite for subsequent clinical application. Solving these questions is fundamental in the development of the product, since the ultimate goal of these products concerns medical application. In addition, the process of purification and sterilization by autoclaving does not remove products and subproducts that are toxic to tissues, mainly endotoxin, lipopolysaccharide (LPS), present on Gram-negative bacteria. However, it is necessary for the process of chemical purification for BC membranes.

Therefore, the importance of such composites for medicine today and the weaknesses presented by these methodologies described in the literature, have prompted us to develop an alternative methodology, more efficient and economically viable for the preparation of composites based on BC and collagen. Thus, in this paper the composites based on BC and collagen were developed with collagen molecules covalently and homogeneously linked to previously purified BC; so, the amount of incorporated collagen can be controlled, and therefore this incorporation can be standardized. Moreover, the results permitted us to conclude that gamma radiation is an adequate treatment for sterilization.

Epifluorescence revealed that at day 1 cells adhered to both BC and BC-COL membrane surfaces, and were mainly round in shape (Fig. 9A and B). At day 3, the cells exhibited a well-spread morphology and some of them showed typical shapes of directional cell movement (Fig. 9C and D). At day 7, BC and BC-COL showed cell confluence and areas of cell multilayering (Fig. 9E and F). The MTT assay indicated no differences between groups at day 10 ($P = 0.2482$) and 14 ($P = 0.0833$) (Fig. 10A). While at day 14 no changes were detected between BC and BC-COL in terms of the total protein content and ALP activity ($P = 0.1489$ and $P = 0.7728$, respectively), at day 17 higher values were observed for BC-COL ($P = 0.0433$ and $P = 0.0209$, respectively) (Fig. 10B and C). At day 21, the calcium content was higher for cultures grown on BC ($P = 0.0209$) (Fig. 10D).

Despite this, epifluorescence and MTT analysis indicated that collagen coating of BC membrane did not affect cell adhesion and proliferation. These results are in agreement with the study by Becker *et al.*,[49] which demonstrated that type I collagen-coated titanium alloy has no effect on osteoblastic cell proliferation.[49] Additionally, a reduced growth rate of rat calvarial bone-derived cells was described for cultures grown on collagen as compared to those grown on plastic.[50] However, BC-collagen composites promoted slight increase in cell adhesion and proliferation in terms of 3T3 fibroblast cell culture;[4] moreover, BC-collagen composites were able to significantly reduce the proteases amount, interleukin concentration and ROS (reactive oxygen species) activity on cell cultures.[5] On the other hand, an *in vitro* study demonstrated that the osteoblastic cells on BC membrane were more sensitive in cytotoxicity assays than the L929 fibroblast cell cultures;[51] which can justify the delay in cell spreading observed in this study for cultures grown on BC and BC-COL membranes in the early periods of culture. Therefore, the BC-COL composite could favor tissue repair for as bone tissue as soft tissues. In addition, BC membranes when functionalized with OGP or OGP[10–14] peptides demonstrated no *in vitro* cytotoxicity, genotoxicity or mutagenicity effects, and additionally the peptides influenced osteogenic cell proliferation, conferring an osteoinductive property to the BC membrane.[52]

Alkaline phosphatase is a membrane-bound enzyme widely recognized as an early marker of osteoblastic differentiation.[53] During bone matrix mineralization, ALP generates the inorganic phosphate needed for hydroxyapatite crystallization and might

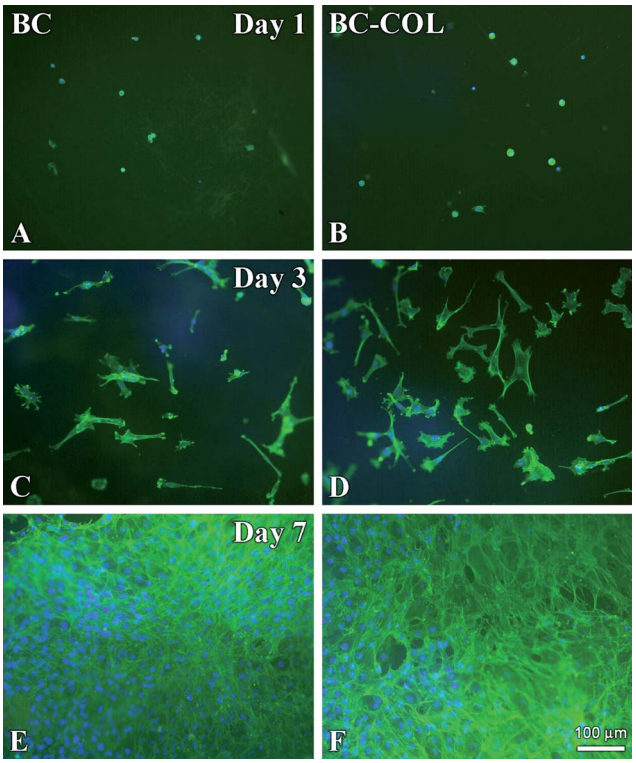

Fig. 9 Epifluorescence of osteoblastic cells cultured on BC (A, C and E) and BC-COL (B, D and F) at 1 (A and B), 3 (C and D) and 7 (E and F) days. Green fluorescence (Alexa Fluor 488-conjugated phalloidin) reveals actin cytoskeleton, whereas blue fluorescence (DAPI DNA stain) highlights cell nuclei. At day 1, the cells adhered and exhibited a roundish shape on both membranes (A and B). At day 3, cell spreading was clearly noticed for both BC and BC-COL (C and D). At day 7, BC and BC-COL showed cell confluence and areas of cell multilayering (E and F). Bar: A–F = 100 μm.

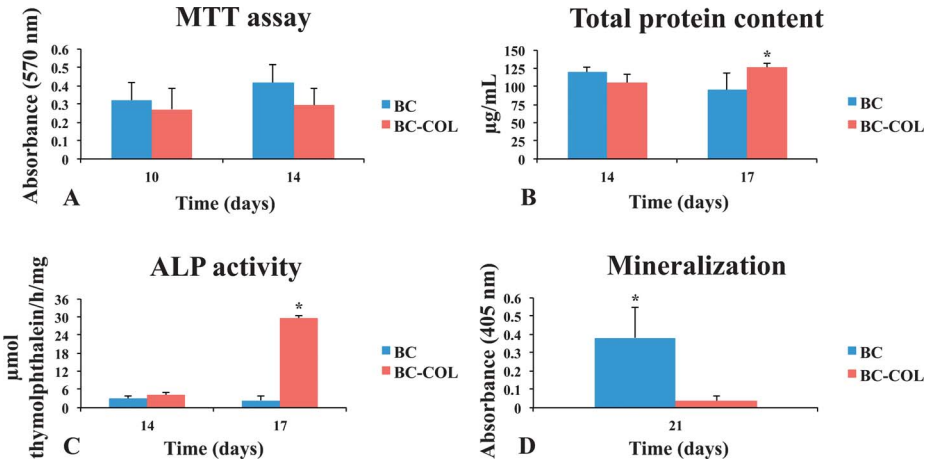

Fig. 10 Osteoblastic cells cultured on BC and BC-COL. Cell viability/proliferation (A) was expressed as absorbance at 10 and 14 days. Total protein content (B) was expressed as milligrams of protein per milliliter at 14 and 17 days. ALP activity (C) was expressed as micromol of thymolphthalein per hour per milligram of protein at 14 and 17 days. Mineralization (D) was expressed as absorbance at day 21. Data are reported as mean ± SD. Asterisks (*) indicate $P < 0.05$ for comparisons between BC and BC-COL at the same time point.

also hydrolyze pyrophosphate, a mineralization inhibitor, to facilitate mineral precipitation and growth.[54] In the present study, although significantly higher values for ALP activity were detected in cultures grown on BC-COL at day 17, the quantitative analysis for matrix mineralization revealed a higher osteogenic potential for the BC membrane. Supporting these results, the lack of correlation between ALP activity and mineralized matrix formation for osteogenic primary cultures has been described elsewhere.[55] Due to the benefits of collagen incorporation into BC in terms of its mechanical properties, but not for the process of matrix mineralization, surface functionalization of BC-COL with other proteins and/or peptides known to promote the acquisition of the osteogenic phenotype should be taken into consideration as a key strategy for the development of BC membranes.

4. Conclusion

The BC-COL composites exhibited a homogeneous nanostructure with a standardized concentration of collagen. These composites have a more flexible structure than BC membranes even after gamma radiation, suggesting that BC-COL might be easier to manipulate during surgical procedures. Additionally, although the matrix mineralization delay obtained for BC-COL, this membrane showed osteoblastic differentiation, as judged by higher levels of ALP activity. The application of strategies to functionalize BC-COL with other proteins and/or peptides that promote bone formation represents the next step in the development of BC-based membranes for bone engineering/regeneration procedures.

Acknowledgements

This work was supported by grants from the Brazilian agencies FAPESP (grant numbers: 08-58776-6 and 09/09960-1) and CNPq. The authors wish to thank Prof. Dr Luiz Geraldo Vaz of Department of Dental Materials and Prosthodontics, Dental School at Araraquara – UNESP for support in the mechanical tests and Mr Roger Rodrigues Fernandes for technical support.

References

1 R. Valentine, P. J. Wormald and R. Sindwani, *Otolaryngol. Clin. North Am.*, 2009, **42**, 813.
2 D. Klemm, B. Heublein, H. P. Fink and A. Bohn, *Angew. Chem., Int. Ed.*, 2005, **44**, 3358.
3 W. K. Czaja, D. J. Young, M. Kawecki and R. M. Brown, *Biomacromolecules*, 2007, **8**, 1.
4 C. Zhijiang and Y. Guang, *J. Appl. Polym. Sci.*, 2011, **120**, 2938.
5 C. Wiegand, P. Elsner, U. C. Hipler and D. Klemm, *Cellulose*, 2006, **13**, 689.
6 H. L. Luo, G. Y. Xiong, Y. Huang, F. He, W. Wang and Y. Z. Wan, *Mater. Chem. Phys.*, 2008, **110**, 193.
7 S. Saska, A. M. M. Gaspar, Y. Messaddeq, S. J. L. Ribeiro, R. Marchetto, *BR Pat.*, 018100019682, 2010; *WO Pat.*, 2011150482-A1, 2011.
8 T. Kokubo, H. Kushitani, S. Sakka, T. Kitsugi and T. Yamamuro, *J. Biomed. Mater. Res.*, 1990, **24**, 721.
9 A. Nanci, S. Zalzal, Y. Gotoh and M. D. McKee, *Microsc. Res. Tech.*, 1995, **33**, 214.
10 J. Moura, L. N. Teixeira, C. Ravagnani, O. Peitl, E. D. Zanotto, M. M. Beloti, H. Panzeri, A. L. Rosa and P. T. de Oliveira, *J. Biomed. Mater. Res., Part A*, 2007, **82**, 545.
11 K. Irie, S. Zalzal, H. Ozawa, M. D. McKee and A. Nanci, *Anat. Rec.*, 1998, **252**, 554.
12 P. T. de Oliveira and A. Nanci, *Biomaterials*, 2004, **25**, 403.
13 T. Mosmann, *J. Immunol. Methods*, 1983, **65**, 55.
14 O. H. Lowry, N. J. Rosebrough, A. L. Farr and R. J. Randall, *J. Biol. Chem.*, 1951, **193**, 265.
15 L. C. Winter, J. A. Gilbert, S. H. Elder and J. D. Bumgardner, *Ann. Biomed. Eng.*, 2002, **30**, 1242.
16 M. A. de Oliva, W. M. Maximiano, L. M. de Castro, P. E. da Silva, Jr, R. R. Fernandes, P. Ciancaglini, M. M. Beloti, A. Nanci, A. L. Rosa and P. T. de Oliveira, *J. Histochem. Cytochem.*, 2009, **57**, 265.
17 C. A. Gregory, W. G. Gunn, A. Peister and D. J. Prockop, *Anal. Biochem.*, 2004, **329**, 77.
18 H. S. Barud, A. M. de Araujo, D. B. Santos, R. M. N. de Assuncao, C. S. Meireles, D. A. Cerqueira, G. Rodrigues, C. A. Ribeiro, Y. Messaddeq and S. J. L. Ribeiro, *Thermochim. Acta*, 2008, **471**, 61.
19 L. J. Zhang, X. S. Feng, H. G. Liu, D. J. Qian, L. Zhang, X. L. Yu and F. Z. Cui, *Mater. Lett.*, 2004, **58**, 719.
20 J. H. Song, H. E. Kim and H. W. Kim, *J. Biomed. Mater. Res., Part B*, 2007, **83**, 248.
21 J. H. Wiley and R. H. Atalla, *Carbohydr. Res.*, 1987, **160**, 113.

22 K. Schenzel, S. Fischer and E. Brendler, *Cellulose*, 2005, **12**, 223.
23 G. Socrates, in *Infrared and Raman Characteristic Group Frequencies: Tables and Charts*, John Wiley & Sons, New York, 2001.
24 Y. Z. Wan, Y. Huang, C. D. Yuan, S. Raman, Y. Zhu, H. J. Jiang, F. He and C. Gao, *Mater. Sci. Eng., C*, 2007, **27**, 855.
25 N. Roveri, G. Falini, M. C. Sidoti, A. Tampieri, E. Landi, M. Sandri and B. Parma, *Mater. Sci. Eng., C*, 2003, **23**, 441.
26 H. S. Barud, C. A. Ribeiro, M. S. Crespi, M. A. U. Martines, J. Dexpert-Ghys, R. F. C. Marques, Y. Messaddeq and S. J. L. Ribeiro, *J. Therm. Anal. Calorim.*, 2007, **87**, 815.
27 C. Gao, G. Y. Xiong, H. L. Luo, K. J. Ren, Y. Huang and Y. Z. Wan, *Cellulose*, 2010, **17**, 365.
28 S. N. Park, J. C. Park, H. O. Kim, M. J. Song and H. Suh, *Biomaterials*, 2002, **23**, 1205.
29 V. Charulatha and A. Rajaram, *Biomaterials*, 2003, **24**, 759.
30 C. P. Barnes, C. W. Pemble, D. D. Brand, D. G. Simpson and G. L. Bowlin, *Tissue Eng.*, 2007, **13**, 1593.
31 M. Coïc, V. Placet, E. Jacquet and C. Meyer, *Rev. Stomatol. Chir. Maxillofac.*, 2010, **111**, 286.
32 Y. Honda, S. Kamakura, K. Sasaki and O. Suzuki, *J. Biomed. Mater. Res., Part B*, 2007, **80**, 281.
33 S. A. Hutchens, R. S. Benson, B. R. Evans, C. J. Rawn and H. O'Neill, *Cellulose*, 2009, **16**, 887.
34 G. Q. Chen and Q. Wu, *Biomaterials*, 2005, **26**, 6565.
35 H. Yu, H. W. Matthew, P. H. Wooley and S. Y. Yang, *J. Biomed. Mater. Res., Part B*, 2008, **86**, 541.
36 G. B. C. Cardoso, A. C. D. Ramos, O. Z. Higa, C. A. C. Zavaglia and A. C. F. Arruda, *J. Mater. Sci.*, 2010, **45**, 4990.
37 F. L. Forti, M. R. Bet, G. Goissis and A. M. G. Plepis, *J. Mater. Sci.: Mater. Med.*, 2011, **22**, 1.
38 F. T. Rodrigues, V. C. A. Martins and A. M. G. Plepis, *Polímeros*, 2010, **20**, 92.
39 G. Goissis, L. Piccirili, J. C. Goes, A. M. D. G. Plepis and D. K. Das-Gupta, *Artif. Organs*, 1998, **22**, 203.
40 S. Yunoki, N. Nagai, T. Suzuki and M. Munekata, *J. Biosci. Bioeng.*, 2004, **98**, 40.
41 Y. Marois, N. Chakfe, X. Deng, M. Marois, T. How, M. W. King and R. Guidoin, *Biomaterials*, 1995, **16**, 1131.
42 L. F. Wolff and B. Mullally, *Int. Dent. J.*, 2000, **50**, 235.
43 D. W. Hutmacher, *Biomaterials*, 2000, **21**, 2529.
44 J. J. Lee, H. S. Yu, S. J. Hong, I. Jeong, J. H. Jang and H. W. Kim, *J. Mater. Sci.: Mater. Med.*, 2009, **20**, 1927.
45 G. Juodzbalys, A. M. Raustia and R. Kubilius, *J. Oral Rehabil.*, 2007, **34**, 781.
46 E. H. Caporali, S. C. Rahal, J. Morceli, R. Taga, J. M. Granjeiro, T. M. Cestari, M. J. Mamprim and M. A. Correa, *Acta Cirurgica Brasileira*, 2006, **21**, 366.
47 C. J. Grande, F. G. Torres, C. M. Gomez and M. C. Bano, *Acta Biomater.*, 2009, **5**, 1605.
48 S. Saska, H. S. Barud, A. M. M. Gaspar, R. Marchetto, S. J. L. Ribeiro and Y. Messaddeq, *Int. J. Biomater.*, 2011, DOI: 10.1155/2011/175362.
49 D. Becker, U. Geissler, U. Hempel, S. Bierbaum, D. Scharnweber, H. Worch and K. W. Wenzel, *J. Biomed. Mater. Res.*, 2002, **59**, 516.
50 M. P. Lynch, J. L. Stein, G. S. Stein and J. B. Lian, *Exp. Cell Res.*, 1995, **216**, 35.
51 Y. M. Chen, T. F. Xi, Y. D. Zheng, T. T. Guo, J. Q. Hou, Y. Z. Wan and C. Gao, *J. Bioact. Compat. Polym.*, 2009, **24**, 137.
52 S. Saska, R. M. Scarel-Caminaga, L. N. Teixeira, L. P. Franchi, R. A. dos Santos, A. M. M. Gaspar, P. T. de Oliveira, A. L. Rosa, C. S. Takahashi, Y. Messaddeq, S. J. L. Ribeiro and R. Marchetto, *J. Mater. Sci.: Mater. Med.*, 2012, **23**, 2253.
53 G. Karsenty, *Front. Biosci.*, 1998, **3**, d834.
54 E. Bonucci, in *Biological Calcification: Normal and Pathological Processes in the Early Stages*, Springer, Berlin-Heidelberg, 2007, pp. 491–506.
55 C. D. Hoemann, H. El-Gabalawy and M. D. McKee, *Pathol. Biol.*, 2009, **57**, 318.

